

Light Scattering by Bent Cylindrical Fibers for Fiber Length and Diameter Characterization

Roman Schuh*, Thomas Wriedt**

(Received: 25 April 2003; in revised form: 23 June 2003; accepted: 30 June 2003)

Abstract

Light scattering computations for cylindrical fibers of high aspect ratios are needed in designing instruments for the optical characterization of airborne fibers. Long airborne fibers may also appear in a bent shape. In this

paper computational results for bent fibers of various radii of bending will be presented using the multiple multipole technique (MMP).

Keywords: fibers, light scattering, null-field method, multiple multipole technique

1 Introduction

Airborne mineral, glass or asbestos fibers are believed to cause serious health hazards. According to the World Health Organization (WHO) fibers are considered dangerous if the diameter is less than 3 μm and the length is more than 5 μm . Additionally, the length to diameter ratio should be higher than 3:1 [1].

The most common method for characterizing airborne fibers is based on the collection of the fibers on a filter and visual inspection of part of the filter by electron microscopy. As this method is quite laborious and time consuming various attempts have been made to develop online instruments using optical methods for fiber characterization [2]. To develop such an instrument light scattering computations for fibers having a high aspect ratio are needed.

Standard methods suitable for this, like the discrete dipole approximation (DDA) and the finite difference time domain (FDTD) are time consuming [3] and other methods like the T-matrix method tend to fail with aspect ratios of higher than about 5:1 [4]. Recently, in this laboratory, both the discrete sources method and null-field method were developed with discrete sources for light scattering computation of fibers having an aspect ratio as high as 100:1 [5, 6]. In both cases the scattering fibers are rotationally symmetric, these methods are not

suitable for performing scattering simulations on bent fibers. For this the multiple multipole technique is used. The book/software package used is the second version of 3D MMP published by Hafner and Bomholt [7]. This release is out of print but the latest version of 3D MMP is included in the upgrade of the MaX-1 software by Hafner [8]. More information on the capability and the history of the MMP method can be found in an overview by Hafner [9].

This method was recently applied to compare the Fraunhofer diffraction of a fiber to exact simulation results [10]. In this paper, an aspect ratio of 4:1 was achieved using the multiple multipole technique. A related problem, scattering by a lossy, dielectric cylinder, which is intended to represent a simplified man model was investigated by Klaus [11].

In the present paper an extension of the multiple multipole technique to fibers having an aspect ratio of 10:1 and also computational results for bent fibers are presented. The paper is divided as follows. In the first part of the paper the theory of the multiple multipole technique is presented. The full theory can be found in Hafner and Bomholt [7] (and references therein). The next part of the paper shows the computation of light scattering by highly elongated straight cylindrical fibers. In this part, computational results obtained by the null-field method with discrete sources are used to validate the results computed using MMP. In the following part computational results for bent fibers of various radii of bending will be presented. Furthermore, differences in the scattering diagrams compared to a straight fiber will be shown.

* Dipl.-Phys. R. Schuh, University of Bremen, FB4 Verfahrenstechnik, Badgasteiner Str. 3, 28359 Bremen (Germany).

** Dr.-Ing. T. Wriedt, Institut für Werkstofftechnik, Badgasteiner Str. 3, 28359 Bremen (Germany).
E-mail: thw@iwt.uni-bremen.de

2 Multiple Multipole Technique

The multiple multipole technique (MMP) is one of the powerful numerical methods called the generalized multipole technique (GMT). The state of the art of GMT is reviewed in an edited volume [12] published recently. MMP was developed by Hafner and co-workers [7] for general electromagnetic computations. The FORTRAN program, provided with this book, is used for this investigation. It is a semi-analytical method, in the sense that the electromagnetic fields are expressed as a linear combination of multiple multipoles, while the amplitudes of the multipoles are obtained by enforcing the boundary conditions in a set of matching points on the surface of the scattering body.

The scattering of electromagnetic waves by a dielectric particle (D_i) with a boundary S and exterior D_s (Figure 1) may be formulated in terms of the following boundary value problem: given $\mathbf{E}_0, \mathbf{H}_0$ in D_s as an entire solution for the Maxwell equations, find the scattered electromagnetic field $\mathbf{E}_s, \mathbf{H}_s$ in D_s and the internal electromagnetic field $\mathbf{E}_i, \mathbf{H}_i$ in D_i satisfying the Maxwell equations

$$\begin{aligned} \nabla \times \mathbf{E}_i - jk_0 \mu_i \mathbf{H}_i &= 0 \\ \nabla \times \mathbf{H}_i - jk_0 \varepsilon_i \mathbf{E}_i &= 0 \end{aligned} \quad (1)$$

and the boundary condition at the interface

$$\begin{aligned} \mathbf{n} \times \mathbf{E}_i - \mathbf{n} \times \mathbf{E}_s - \mathbf{n} \times \mathbf{E}_0 &= 0, \\ \mathbf{n} \times \mathbf{H}_i - \mathbf{n} \times \mathbf{H}_s - \mathbf{n} \times \mathbf{H}_0 &= 0. \end{aligned} \quad (2)$$

The scattered field $\mathbf{E}_s, \mathbf{H}_s$ additionally has to fulfill the Silver Müller radiation condition at infinity:

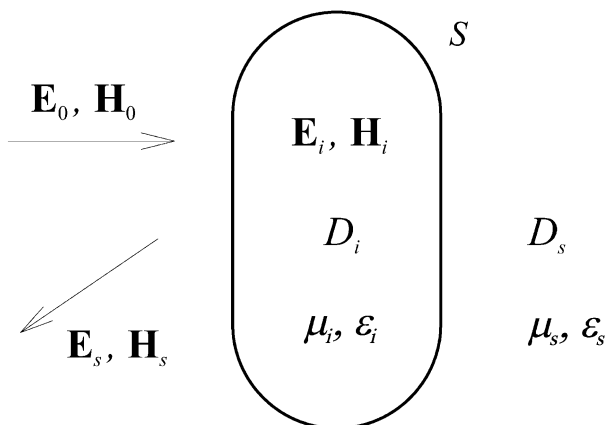


Fig. 1: Illustration of the basic MMP model variables.

$$\frac{\mathbf{x}}{|\mathbf{x}|} \times \sqrt{\mu_s} \mathbf{H}_s + \sqrt{\varepsilon_s} \mathbf{E}_s = o\left(\frac{1}{|\mathbf{x}|}\right), \quad (3)$$

as $|\mathbf{x}| \rightarrow \infty$, uniformly for all directions $\frac{\mathbf{x}}{|\mathbf{x}|}$.

Index t is defined as $t = s, i$; μ_t and ε_t are the permeability and the permittivity of domain D_t , respectively, k_0 denotes the wavenumber in D_s and \mathbf{n} is the unit outward normal vector on S .

An approximate solution $\mathbf{E}_t^N, \mathbf{H}_t^N$ of the scattering problem is constructed as a finite linear combination of fields of multiple multipoles having different origins. For the scattered field these multipoles will be located inside D_i , so that $\mathbf{E}_s^N, \mathbf{H}_s^N$ is a radiating solution to the Maxwell equations being regular in D_s . For the internal field $\mathbf{E}_i^N, \mathbf{H}_i^N$ the radiating multipoles will be located in D_s , while the regular ones are located in D_i . The origins of the multipoles are distributed according to the shape of the scattering domain.

It can be shown [13], that the following estimate holds for the approximate solution of the scattering problem:

$$\begin{aligned} &\|\mathbf{E}_s - \mathbf{E}_s^N\|_{\infty, G_s} + \|\mathbf{H}_s - \mathbf{H}_s^N\|_{\infty, G_s} + \|\mathbf{E}_i - \mathbf{E}_i^N\|_{\infty, G_i} \\ &+ \|\mathbf{H}_i - \mathbf{H}_i^N\|_{\infty, G_i} \leq C (\|\mathbf{n} \times \mathbf{E}_s^N + \mathbf{n} \times \mathbf{E}_0 - \mathbf{n} \times \mathbf{E}_i^N\|_{2, S} \\ &+ \|\mathbf{n} \times \mathbf{H}_s^N + \mathbf{n} \times \mathbf{H}_0 - \mathbf{n} \times \mathbf{H}_i^N\|_{2, S}), \end{aligned} \quad (4)$$

where $G_s \subset D_s, G_i \subset D_i$ and C is a constant depending on G_t and S .

According to the above estimate a quasi-solution to the boundary value condition can be obtained by approximating the tangential components of the incident fields $\mathbf{E}_0, \mathbf{H}_0$ on the boundary of the scatterer by multiple multipoles. For estimate (4) to be valid the system of multiple multipoles is required to be complete, which has been proven by Doicu et al. [14].

The implementation of MMP into a numerical algorithm for calculation of the fields of a dielectric scatterer is done the following way. Let

$$\begin{aligned} \mathcal{M}_{mnp}^{3t} &= \mathbf{M}_{mn}^{3t} [k_t (\mathbf{x} - \mathbf{x}_{0p})], \\ \mathcal{N}_{mnp}^{3t} &= \mathbf{N}_{mn}^{3t} [k_t (\mathbf{x} - \mathbf{x}_{0p})], \end{aligned} \quad (5)$$

be the radiating spherical vector wave functions with their singularities located at \mathbf{x}_{0p} such that the system $\{\mathbf{n} \times \mathcal{M}_{mnp}^{3t}, \mathbf{n} \times \mathcal{N}_{mnp}^{3t}\}$ is linearly independent and complete on S . $\{\mathcal{M}_{mnp}^{3t}, \mathcal{N}_{mnp}^{3t}\}$ of course fulfill the Maxwell equations. Index p denotes the number of the multipole, $k_t = k_0 \sqrt{\varepsilon_t \mu_t}$ is the wavenumber of the domain D_t and \mathbf{M}_{mn}^{3t} and \mathbf{N}_{mn}^{3t} are defined as

$$\mathbf{M}_{mn}^{3r} = h_n(k_r r) \left[jm \frac{P_n^{(m)}(\cos\theta)}{\sin\theta} \mathbf{e}_\theta - \frac{dP_n^{(m)}(\cos\theta)}{d\theta} \mathbf{e}_\varphi \right] e^{jm\varphi},$$

$$\mathbf{N}_{mn}^{3r} = \left\{ \begin{array}{l} n(n+1) \frac{h_n(k_r r)}{k_r r} P_n^{(m)}(\cos\theta) \mathbf{e}_r \\ + \frac{[k_r r h_n(k_r r)]'}{k_r r} \left[\frac{dP_n^{(m)}(\cos\theta)}{d\theta} \mathbf{e}_\theta \right. \\ \left. + jm \frac{P_n^{(m)}(\cos\theta)}{\sin\theta} \mathbf{e}_\varphi \right] \end{array} \right\} e^{jm\varphi}, \quad (6)$$

where $(\mathbf{e}_r, \mathbf{e}_\varphi, \mathbf{e}_\theta)$ are the unit vectors in spherical coordinates, n is the order of the multipole, m is the azimuthal mode, h_n denotes the Hankel function and $P_n^{(m)}$ the Legendre polynomials.

The approximate internal and scattered electric fields \mathbf{E}_i^N are represented as a linear combination of radiating spherical vector wave functions with P different poles

$$\mathbf{E}_s^N = \sum_{p=1}^P \sum_{n=1}^{N_p} \sum_{m=-n}^n a_{mnp}^N \mathcal{M}_{mnp}^{3s} + b_{mnp}^N \mathcal{N}_{mnp}^{3s}, \quad (7)$$

$$\mathbf{E}_i^N = \sum_{p=1}^P \sum_{n=1}^{N_p} \sum_{m=-n}^n c_{mnp}^N \mathcal{M}_{mnp}^{3i} + d_{mnp}^N \mathcal{N}_{mnp}^{3i}. \quad (8)$$

The expansion coefficients a_{mnp}^N , b_{mnp}^N , c_{mnp}^N , and d_{mnp}^N are obtained by minimizing the residual field:

$$\mathbf{a} = \arg \min \left\{ \left\| \mathbf{n} \times \mathbf{E}_s^N + \mathbf{n} \times \mathbf{E}_0 - \mathbf{n} \times \mathbf{E}_i^N \right\|_{2,S}^2 + \left\| \mathbf{n} \times \mathbf{H}_s^N + \mathbf{n} \times \mathbf{H}_0 - \mathbf{n} \times \mathbf{H}_i^N \right\|_{2,S}^2 \right\}, \quad (9)$$

where $\mathbf{a} = [a_{mnp}^N, b_{mnp}^N, c_{mnp}^N, d_{mnp}^N]^T$. While the approximate solution \mathbf{E}_i^N , \mathbf{H}_i^N converges to the exact solution \mathbf{E}_i , \mathbf{H}_i ; the relative error may be computed by

$$\varepsilon_N = \frac{\left\| \mathbf{n} \times \mathbf{E}_s^N + \mathbf{n} \times \mathbf{E}_0 - \mathbf{n} \times \mathbf{E}_i^N \right\|_{2,S} + \left\| \mathbf{n} \times \mathbf{H}_s^N + \mathbf{n} \times \mathbf{H}_0 - \mathbf{n} \times \mathbf{H}_i^N \right\|_{2,S}}{\left\| \mathbf{n} \times \mathbf{E}_0 \right\|_{2,S} + \left\| \mathbf{n} \times \mathbf{H}_0 \right\|_{2,S}}. \quad (10)$$

In order to reduce the computational effort, the surface of the scatterer has to be discretized in a set of J matching points. Thus the integrals appearing in (9) are approximated by a numerical scheme and the expansion coefficients may formally be written as the solution of the least square problem:

$$\mathbf{a} = \arg \min \left\| \mathbf{A} \mathbf{x} - \mathbf{f} \right\|_r^2 \quad (11)$$

where the matrix \mathbf{A} and the vector \mathbf{f} depend on the values of the spherical vector wave functions and the incident

field at the matching points, respectively. \mathbf{A} is a rectangular matrix with the number of matching points J being larger than the number of multipoles. Equation (11) is solved by using QR decomposition with an algorithm based on Givens rotations.

Because the origin of multipoles can be set very flexibly, MMP is able to calculate the field of arbitrarily shaped objects, especially cylinders with large aspect ratios. The computation time for the fibers presented in the following sections is about 2 h using a Compaq ES20 computer (Alpha processor, 667 MHz). The number of matching points of the model amounts to 2554 and the number of multipoles for both the internal and the external fields is 17. For this configuration, the current upper limit for MMP calculations for fibers lies at a fiber length of about 10 μm for a wavelength of $\lambda = 514.5\text{nm}$. This limitation is mainly due to immense memory demand and rising numerical instabilities. Scattering by larger objects with the restriction to rotational symmetry can be computed using the recently developed extension of the null-field method with discrete sources [6].

3 Scattering by Straight Fibers: Comparison of Numerical Results

In this section computational results for a particle, whose shape is best described as a fiber with rounded ends, is presented. The ends of this fiber are modeled as half spheres. It was found that fibers with rounded ends are most suitable for use with the MMP program. The model of the fiber is shown in Figure 2.

The aspect ratio of the particle is $a:b=10:1$. The size parameters of the particle are defined by ka and kb , with the wavenumber $k = 2\pi/\lambda$ and $2a$ and $2b$ the length and width of the particle, respectively. The refractive index is $n = 1.5$. The differential scattering cross sections (DSCS) computed with the multiple multipole technique (MMP) and the null-field method with discrete sources (NFM-DS) were compared for different size and orientation of the particle. In the

NFM-DS distributed lowest order spherical vector wave functions are distributed on the symmetry axis of the fiber for internal field representation. For external field expansion a set of spherical vector wave functions is positioned at the center of the fiber. A similar approach, taking account of rotational symmetry, was used by Klaus [11] in the first version of MMP. In our MMP model the multipoles are positioned on the symmetry axis for both the internal and the external fields. For the straight fiber and perpendicular incident light it is possible to take advantage of three reflective symmetries

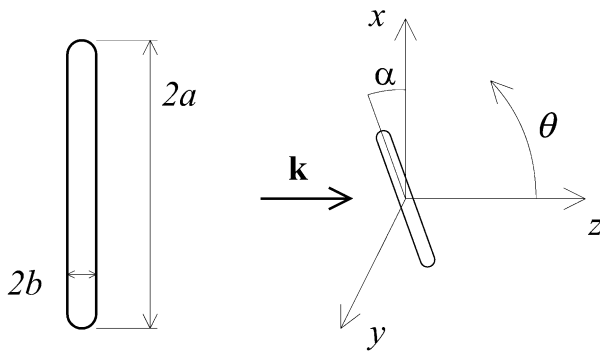


Fig. 2: Model of the simulated fiber. The aspect ratio is $a:b = 10:1$.

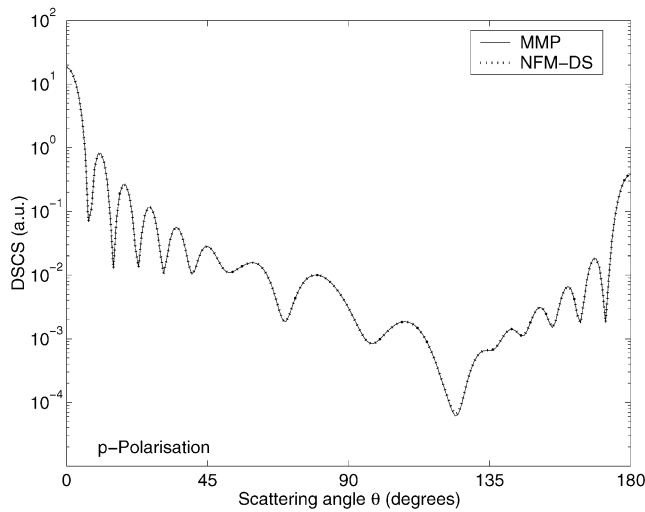


Fig. 3: Computed DSCS of a fiber at $\alpha=0^\circ$ and parallel polarization ($ka = 8\pi = 25.13$, $kb = 8\pi/10 = 2.513$).

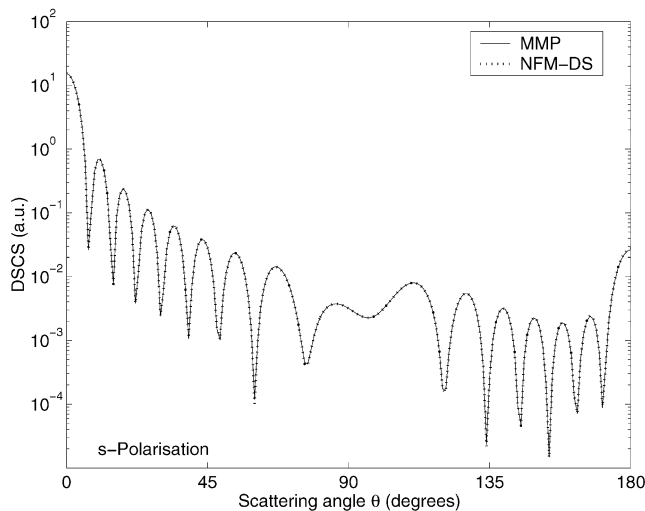


Fig. 4: Computed DSCS of a fiber at $\alpha=0^\circ$ and perpendicular polarization ($ka = 8\pi = 25.13$, $kb = 8\pi/10 = 2.513$).

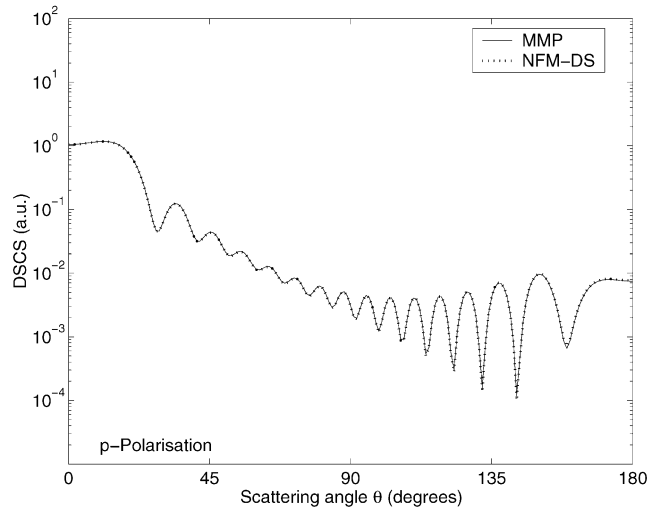


Fig. 5: Computed DSCS of a fiber at $\alpha=90^\circ$ and parallel polarization ($ka = 8\pi = 25.13$, $kb = 8\pi/10 = 2.513$).

with respect to the three perpendicular planes. This leads to a significant reduction in the number of matching points reducing both calculation time and memory requirement.

The incident wave is a linearly polarized plane wave propagating along the z -axis. The scattering characteristics will be displayed in the azimuthal plane $\varphi = 0$.

The first example is a fiber with the geometry of the model shown in Figure 2. The size parameters of the fiber are $ka = 8\pi$ and $kb = 0.8\pi$ with the tilt angle $\alpha = 0^\circ$. The simulation results for parallel polarization are presented in Figure 3 and those for perpendicular polarization are shown in Figure 4.

These two simulations show perfect agreement in the differential scattering cross section. This is mainly achieved by the suitable positioning and adjusting of the order of the multipoles in the MMP simulation. The multipoles are positioned equidistant along the rotational axis with increasing order at the fiber ends.

The next example is the same fiber tilted. The size parameters of the fiber are $ka = 8\pi$ and $kb = 0.8\pi$ with the tilt angle $\alpha = 90^\circ$. The simulation results are presented in Figure 5 for parallel and in Figure 6 for perpendicular polarization.

Both polarization results also show perfect agreement in the differential scattering cross section computed by the different programs.

The next example is the same fiber with a tilt angle $\alpha = 30^\circ$. The size parameters of the fiber are $ka = 8\pi$ and $kb = 0.8\pi$. The simulation results are presented in Figure 7 for parallel and in Figure 8 for perpendicular polarization.

Also, in this case there is perfect agreement between the results obtained by the different programs. Thus, it is

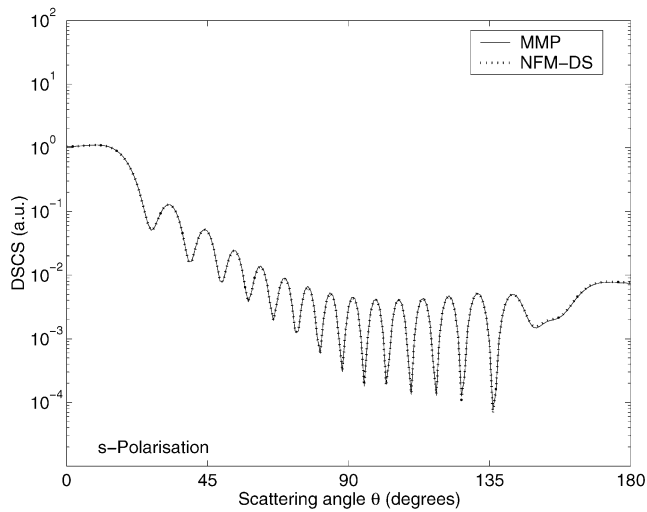


Fig. 6: Computed DSCS of a fiber at $\alpha = 90^\circ$ and perpendicular polarization ($ka = 8\pi = 25.13$, $kb = 8\pi/10 = 2.513$).

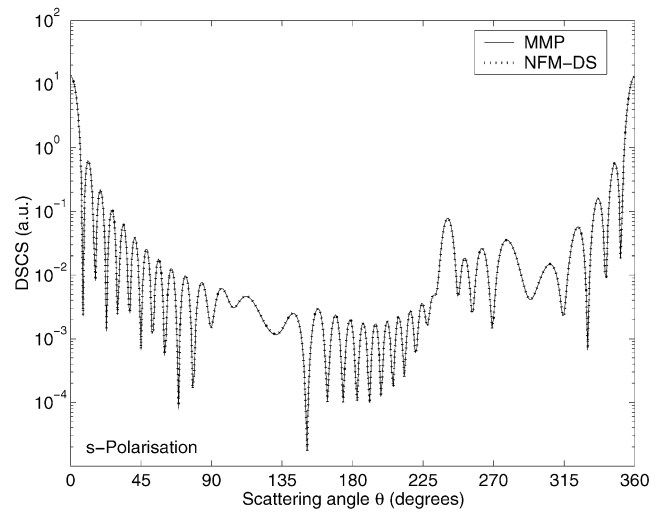


Fig. 8: Computed DSCS of a fiber at $\alpha = 30^\circ$ and perpendicular polarization ($ka = 8\pi = 25.13$, $kb = 8\pi/10 = 2.513$).

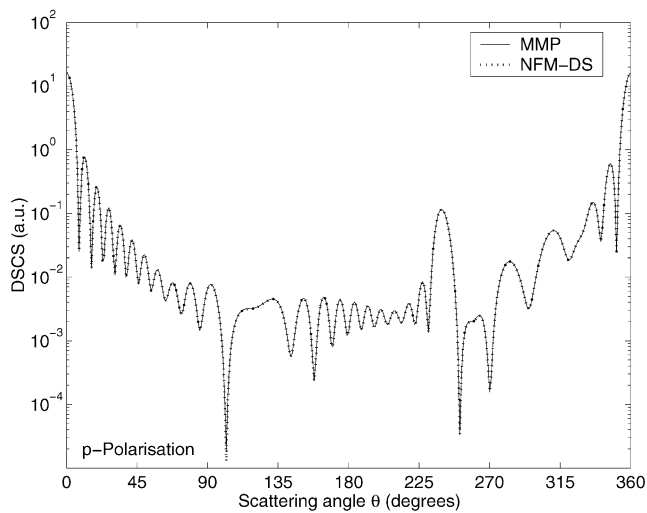


Fig. 7: Computed DSCS of a fiber at $\alpha = 30^\circ$ and parallel polarization ($ka = 8\pi = 25.13$, $kb = 8\pi/10 = 2.513$).

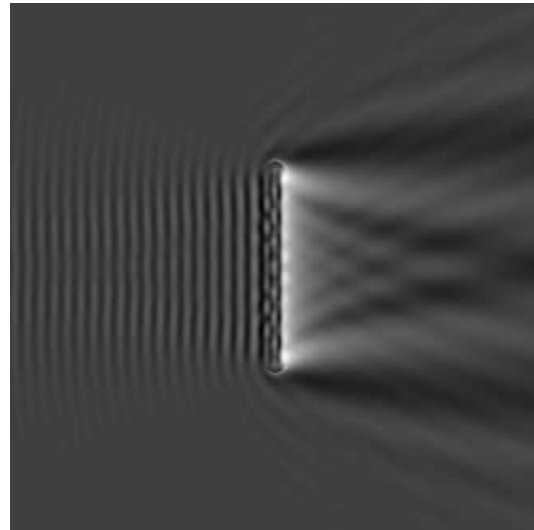


Fig. 9: Near-field intensity distribution: scattering of a perpendicular polarised plane wave by a fiber with $ka = 8\pi$ and $kb = 8\pi/10$, $\alpha = 0^\circ$.

concluded that a suitable strategy is available to place the multipoles in the MMP program in such a way that complicated scattering problems can be solved.

Additionally, with MMP it is possible to compute the fields and intensities in the near-field area. Figure 9 depicts the near-field intensity distribution of a fiber with the parameters $ka = 8\pi$, $kb = 0.8\pi$, $n = 1.5$, $\alpha = 0^\circ$ and perpendicular polarization.

The total intensity is plotted in this image, i.e., the interference of the incident and the scattered light. Because of this, there are interference fringes in the backscattering region. Also, the internal field distribution has been computed and internal oscillations are visible.

4 Scattering by Bent Fibers: Numerical Results

Having tested the MMP adaptation in the previous section, computational results for bent fibers will be presented next. Mineral fibers like asbestos fibers often appear in a bent shape. Straight fibers are expected mostly for small sizes. Light scattering changes with the shape of the fibers (fibers otherwise the same size). For this reason numerical simulations are important for the development of optical characterization methods. In this part the focus is on the changes in light scattering for different radii of bending. For simplification, the fiber is characterized with only one additional parameter, the

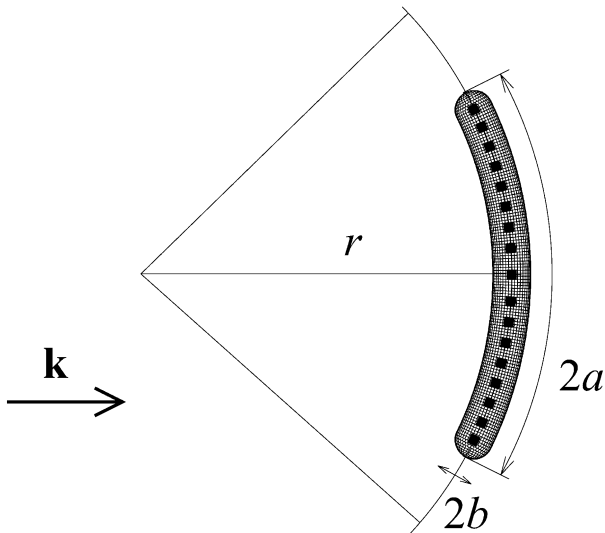


Fig. 10: MMP model of a bent fiber. The fiber is bent along the arc with a radius r . The model shown has a radius of bending of $r = 2a$. The definition of the size parameters a and b is straightforward, see model in Figure 2. The squares along the arc represent the multipoles.

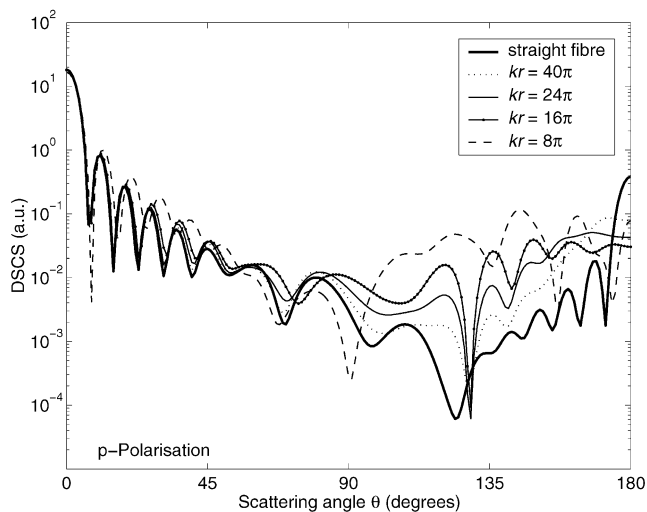


Fig. 11: Computed DSCS of a fiber with different radii of bending at $\alpha = 0^\circ$ and parallel polarization ($ka = 8\pi = 25.13$, $kb = 8\pi/10 = 2.513$).

radius of bending. Every matching point and multipole of the original straight model is moved and rotated according to the radius of bending (Figure 10).

The orders of the multipoles remain unchanged. With the tilt angle α as defined in Figure 2 the bent fiber can be modeled with two reflective symmetries.

Since the null-field method with discrete sources used by Pulbere and Wriedt [6] only allows the multipoles to be set on the rotational axis this method cannot be applied

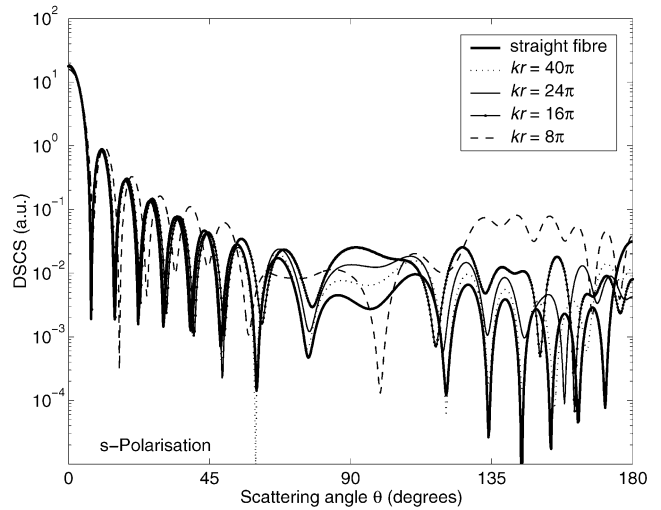


Fig. 12: Computed DSCS of a fiber with different radii of bending at $\alpha = 0^\circ$ and perpendicular polarization ($ka = 8\pi = 25.13$, $kb = 8\pi/10 = 2.513$).

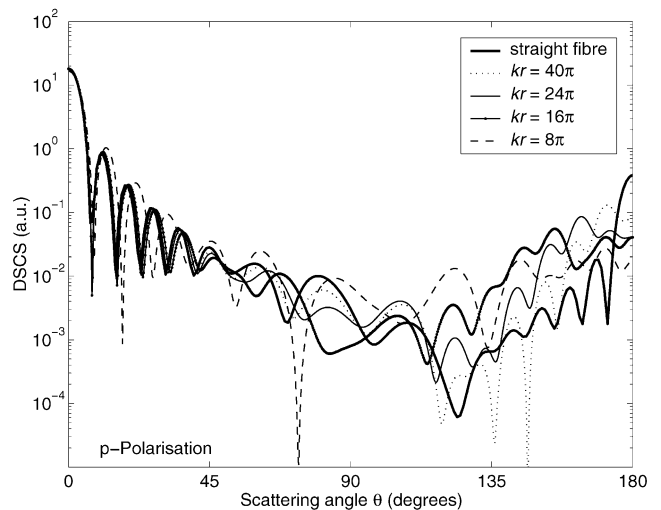


Fig. 13: Computed DSCS of a fiber with different radii of bending at $\alpha = 180^\circ$ and parallel polarization ($ka = 8\pi = 25.13$, $kb = 8\pi/10 = 2.513$).

for bent fibers. All simulations for bent fibers were done with the multiple multipole technique.

Figures 11 and 12 show simulated light scattering by a fiber with different radii of bending.

The incident wave is parallel polarized in Figure 11 and perpendicular in Figure 12. The solid line shows the light scattering from a straight fiber identical to the one from Figure 3. The fiber is bent towards the direction of the incident plane wave. The radius of bending (radius of curvature) is gradually reduced from $kr = \infty$ (straight fiber) to $kr = 8\pi$ (high curvature). The simulation results show that the differences in the DSCS are small in the

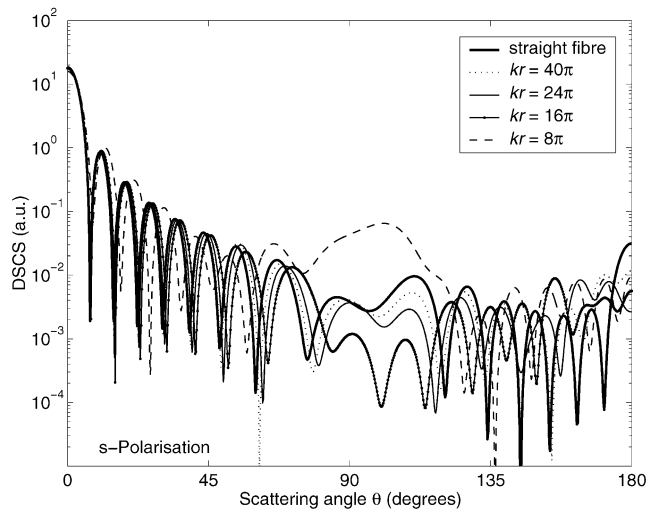


Fig. 14: Computed DSCS of a fiber with different radii of bending at $\alpha = 180^\circ$ and perpendicular polarization ($ka = 8\pi = 25.13$, $kb = 8\pi/10 = 2.513$).

forward direction up to a scattering angle of $\theta = 60^\circ$. The differences in the backward direction are more pronounced. The lower the radius of bending the greater are the differences of DSCS of the fiber compared to the DSCS of the original straight fiber.

Figures 13 and 14 show the scattering of a fiber with a different orientation.

The orientation of the fiber is changed so that $\alpha = 180^\circ$. In this configuration, the fiber is bent away from the direction of the incident plane wave. The incident wave is polarized parallel in Figure 13 and perpendicular in Figure 14. Again, the simulation results show that the differences in the DSCS are small in the forward direction up to a scattering angle of $\theta = 60^\circ$. The differences in the backward direction are more pronounced. This, and numerous further simulations, show that the orientation and the radius of bending of a fiber can have a great effect on the light scattering distribution.

5 Conclusion

The multiple multipole technique (MMP) has been adapted for simulating the light scattering of bent cylindrical fibers. The adapted program has been tested by comparing the results for straight fibers obtained by a program based on the null-field method with discrete sources. It has been demonstrated that the lower the radius of bending the more the scattering diagram differs from a straight fiber. Using such computations, of the

scattering of a bent fiber, in the development of an optical fiber detector it is hoped that it will be possible to differentiate between bent and straight fibers.

6 Acknowledgement

We gratefully acknowledge support for the research from Deutsche Forschungsgemeinschaft (DFG).

7 References

- [1] Kommission Reinhaltung der Luft, *Sicherer Umgang mit Fasermaterialien*, VDI Berichte 1417. VDI Verlag, Düsseldorf, **1998**.
- [2] K. Bauckhage, M. Bottlinger, F. Ebert, H. Fissan, S. Ripperger, K. Sommer, R. Weichert, T. Wriedt, Untersuchungen zur Charakterisierung von Faserkollektiven, in *Sicherer Umgang mit Fasermaterialien*, VDI Berichte 1417, Ed.: Kommission Reinhaltung der Luft. VDI Verlag, Düsseldorf, **1998**, pp. 251–273.
- [3] T. Wriedt, A Review of Elastic Light Scattering Theories. *Part. Part. Syst. Charact.*, **1998**, 15, 67–74.
- [4] M. I. Mishchenko, J. W. Hovenier, L. D. Travis, *Light Scattering by Nonspherical Particles: Theory, Measurements and Applications*. Academic Press, San Diego, **2000**.
- [5] E. Eremina, Y. Eremin, T. Wriedt, Extension of Discrete Sources Method to light scattering by highly elongated finite cylinders. *J. Modern Optics*, submitted for publication.
- [6] S. Pulbere, T. Wriedt, Light Scattering by Cylindrical Fibers with High Aspect Ratio Using Null-Field Method with Discrete Sources. *Part. Part. Syst. Charact.*, submitted for publication.
- [7] C. Hafner, K. Bomholt, *The 3D electrodynamic wave simulator*. Wiley, Chichester, **1993**.
- [8] C. Hafner, MaX-1, A Visual Electromagnetics Platform for PCs, CD-ROM Package. Wiley, Chichester, **2002**.
- [9] C. Hafner, The Multiple Multipole Program (MMP) and the Generalized Multipole Technique (GMT), *Generalized Multipole Techniques for Electromagnetic and light scattering*, Ed.: T. Wriedt. Elsevier, Amsterdam, **1999**, pp. 21–38.
- [10] H. Sagehorn, J. List, T. Wiegand, R. Weichert, T. Wriedt, Characterization of Airborne Fibers via Fraunhofer Theory: Examination of the Validity of Fraunhofer Theory Using the Exact Scattering Theory MMP. *Part. Part. Syst. Charact.*, **2001**, 18, 55–63.
- [11] G. Klaus, *3-D Streufeldberechnungen mit Hilfe der MMP-Methode*. PhD Thesis, ETH Zürich, **1985**.
- [12] T. Wriedt, *Generalized Multipole Techniques for electromagnetic and light scattering*. Elsevier, Amsterdam, **1999**.
- [13] T. Wriedt, A. Doicu, U. Comberg, H. Sagehorn, R. Schuh, Gaussian beam scattering using the discrete sources method, *Scattering of shaped light beams and applications*, Ed.: G. Gouesbet. Research Signpost, Trivandrum, India, **2000**.
- [14] A. Doicu, Y. Eremin, T. Wriedt, *Acoustic and Electromagnetic Scattering Analysis using Discrete Sources*. Academic Press, London, **2000**.